Joint influence of river stream, water level and wind waves on the height of sand bar in a river mouth

J. Laanearu[1], T. Koppel[2], T. Soomere[3] and P.A. Davies[4]

[1]Institute of Mechanics, Tallinn University of Technology, Ehitajate tee 5, Tallinn 19086, Estonia.
E-mail: *janek@staff.ttu.ee*
[2]Department of Civil Engineering, Tallinn University of Technology, Ehitajate tee 5, Tallinn 19086, Estonia
[3]Institute of Cybernetics, Tallinn University of Technology, Ehitajate tee 5, Tallinn 19086, Estonia
[4]Department of Civil Engineering, University of Dundee, Dundee DD1 4HN, UK

Received 23 August 2006; accepted in revised form 13 March 2007

Abstract The hydraulics theory and wind-wave modelling are used to model annual changes of a threshold (sand bar) height at the mouth of the Narva River in 2002. The changes in the threshold height are attributed to two mechanisms: the cross-shore sediment transport driven by the river flow that erodes the obstacle and the long-shore transport forced by waves that increases the threshold height. It is shown that the flow stratification in the river mouth switches between one- and two-layer modes in different seasons, depending on variations of water level, river discharge and wave activity.

Keywords Bottom friction; Froude number; Narva Bay; sand bar; sediment dynamics

Nomenclature

a	significant wave amplitude (resp. half of the significant wave height)
A, A_1	cross-sectional area of the river flow and of the upper layer, respectively
$A_w(\equiv \mathrm{v}/\omega)$	wave-induced bottom excursion amplitude
B_0	dimensionless upstream-section specific energy, $B_{0L} = B_0(L)$
b, $b*$	bottom and interface elevation, respectively
dF_{drag}	boundary drag force per unit mass
D	undisturbed water depth
e_f	efficiency factor of stream power available to move the sediments
f_r, f_w	current (resp. river flow) and wave friction factor, respectively
Fr , F_1	open channel and internal Froude number, respectively
$\vec{g} = (0, 0, -g)$	vector of acceleration due to gravity
$g' = g(1 - r)$	reduced gravity
h_1, h_2	thicknesses of the upper (outflowing) and a lower (arrested)
$h(= h_1(0))$	water depth at the natural river mouth, $h_{1L} = h_1(L)$
k	wavenumber
$k_n = 30\nu/9u_*$	hydraulic roughness
K_1, K_2	morphodynamic coefficients
q_L	dimensionless volume flux
q_{cs}, $q_{\mathrm{v}s}$	cross- and along-shore sediment-volume flux per unit width, respectively
Q_1	volume flux of upper layer
$r(= \rho_1/\rho_2)$	density ratio of the upper, river water (ρ_1) and lower, sea water (ρ_2) layers

Nordic Hydrology **Vol 38 No 3 pp 287–302**

doi: 10.2166/nh.2007.012

$\mathrm{Re}_c, \mathrm{Re}_w$	channel and wave Reynolds number, respectively
R_1	hydraulic radius of the river channel
u_1, u_2	upper- and lower-layer flow velocity, respectively
$u(=u_1(0))$	velocity at the natural river mouth, $u_{1L}=u_1(L)$
u_s, v_s	cross- and along-shore velocity scale of the bulk sediment volume, respectively
u_*	frictional velocity
$Y_s=(\rho_s-\rho)g$	submerged weight of bottom material
$w(x)$	width of channel, $w_L=w(L)$, $w_0=w(0)$
v	maximum wave-induced near-bed orbital velocity
δ	thickness of sediment volume
Δ	maximum height of the sill
ϵ	coefficient of sediment volumetric concentration
φ	angle (clockwise) between the North and the wave propagation direction
Φ ($\tan\Phi$)	angle of repose for the sediment slope (the coefficient of internal friction)
η	surface elevation
ν	coefficient of kinematic viscosity
ρ, ρ_s	water and grain density, respectively
τ_r, τ_w	bottom shear stress due to current and waves, respectively
ω	angular frequency
ς_1, ς_2	operators determining the flow regime

Introduction

Many different hydrodynamic processes are responsible for the enhanced deposition of sediments and the formation of a sand bar at the mouth of an estuary or tidal inlet. Deposition may be promoted naturally (see, for example, Largier *et al.* 1992; Coates *et al.* 2001) either individually or in combination by (i) seasonally low river flows, (ii) upstream abstraction of river water for agricultural or industrial use or (iii) onshore and long-shore transport processes associated with wave, current and tidal action. Not least, sand bars may also form as a result of any anthropogenic activities that affect the natural exchange processes at the estuary mouth.

In the present study, attention is directed towards the roles of river discharge and offshore coastal dynamics in determining the formation of a sand bar at the mouth of an estuary already modified by dredging operations and breakwater construction. The site in question (Figure 1) is the mouth of the River Narva as it enters into the Narva Bay, an open sub-basin of the Baltic Sea in the eastern part of the Gulf of Finland (for details see Alenius *et al.* 1998). The long-term mean of discharge of the river is around 400 $\mathrm{m}^3\ \mathrm{s}^{-1}$, reflecting the confluence of surface water from the catchments area around 56 000 km^2 (Protasjeva and Eipre 1972), though the monthly value can be two times as large during spring floods. The bay is mostly sandy at the coast and is open to the dominating winds (Laanearu and Lips 2003). As a consequence, the Narva River mouth area is an interaction zone between wave- and current-induced sand motions. The sand bar formed in the Narva River mouth presents a highly inconvenient obstacle to ship traffic during relatively low water-level conditions.

Littoral processes near the river mouth are modified by the presence of the Narva-Jõesuu breakwater. This is a structure about 300 m in length and built (i) to facilitate navigation between the harbour and sea and (ii) to prevent extensive beach erosion. The structure is placed approximately perpendicular to the beach, westward from the river mouth (see inset in Figure 1). Together with the natural eastern coastal bank, it forms the outlet for the Narva River. Measurements of the Froude number Fr (see below) at the natural river mouth reveal permanent sub-critical flow conditions, confirming that flow dissipation effects due to

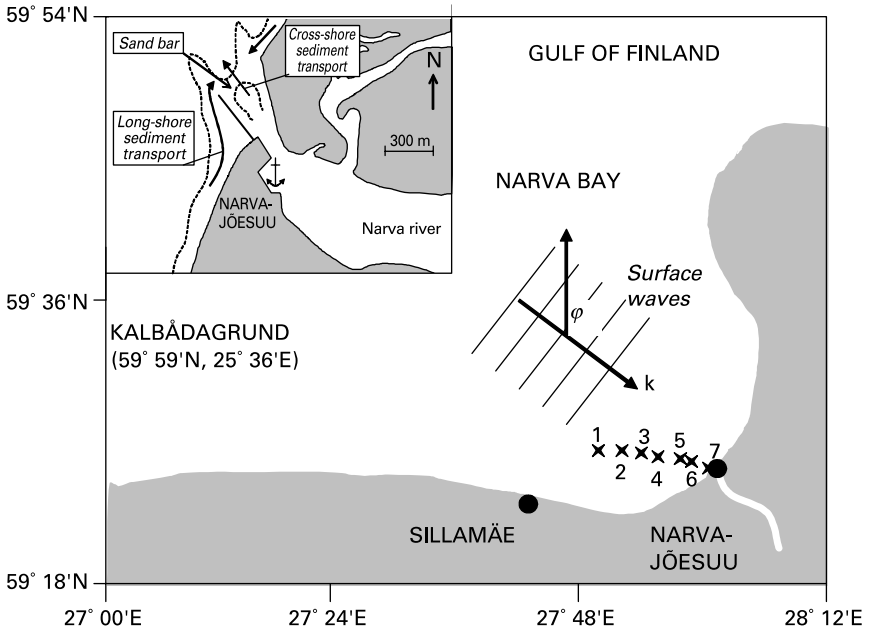

Figure 1 Map of the Narva Bay and a sketch of beach-approaching surface waves (wave vector k and angle of wave propagation direction φ). The Narva River mouth hydrological system and breakwater are shown in the inset. Hydrographical stations (1–7) are indicated by crosses

separation at the sides of the river channel are minor (cf. Kalkwijk and Koppel 1985). The magnitude of the river flow and the morphological changes occurring at the inlet area of the Narva River are tightly related. The water depth is modest (about 2–4 m) in the vicinity of the seaward end of the breakwater, where the sand bar is highest. The depth increases considerably upstream, reaching 8–10 m at the natural river mouth. The mean velocity of the river stream ranges between 0.2 m s^{-1} and 1.0 m s^{-1}. The water depth in the sea increases seawards and reaches 10 m at a point 2 km offshore. In this sense, the flow in the mouth of the Narva River can be classified as sill flow (see, for example, Baines 1998).

For many estuaries, tidal forcing usually determines whether exchange flow exists at the river mouth (Coates *et al.* 2001; Cuthbertson *et al.* 2004); yet the effect of tides is negligible in the whole Baltic Sea (Wübber and Krauss 1979). Coastal currents related to the general circulation of the Gulf of Finland as well as wind-induced, low-frequency motions are only significant for regions away from the Narva River mouth (Laanearu and Lips 2003). Some other factors (such as ridge ice, local near-bottom currents not related to the river discharge and wave-induced cross-shore sand transport) at times influence sand movement, but they are not decisive in the long-term dynamics in the area in question.

In this study hydrophysical and meteorological data collected from the Narva Bay region in 2002 are used to develop and validate a mathematical model for annual changes of the bottom at the mouth of the Narva River resulting from the effects of river outflow and coastal sediment transport processes. The key ideas employed here are that (i) the sand transport is partitioned into two components: the cross-shore transport is driven by the river stream and the long-shore transport is forced by waves, and that (ii) the comparatively slow changes in bottom topography at the river mouth can be treated as a nearly balanced situation between the processes of sand barrier erosion and replenishment. The observed hydrological conditions and the estimated hydraulic parameters suggest that the one-layer hydraulic model clearly fails to describe changes in the bottom topography of the river mouth. Hence,

a two-layer exchange flow approach is adopted to incorporate the observed stratification in the river-mouth area.

The plan of the paper is as follows. The next sction gives the overview of existing hydrological, meteorological, hydrographical measurements and of modelled wave fields, all of which are used as an input of the proposed model. In the third section, the momentum and continuity equations for the river flow are integrated to derive a specific volume-transport equation. The morphodynamic relationships are presented next. Morphological changes affecting the sill height include the erosional processes associated with the river flow above the sill as well as the wave-induced coastal sediment transport leading to gradual filling of the bar area. Observations of the river discharge and results of wave modelling from the second section are next used in to calculate long- and cross-shore bottom stresses, respectively, and to estimate bathymetric changes in the river mouth. The final section contains conclusions and discussion of the results.

Observed river discharge and modelled wave parameters

The outflow conditions from the Narva River are characterized essentially by the discharge and the water level in the Narva-Jõesuu harbour. The temporal variation of these parameters during 2002 are presented in Figure 2. The river hydrograph has a spring maximum and a smaller flux during the rest of the year. The daily maximum and minimum discharge are around 710 $m^3\ s^{-1}$ and 160 $m^3\ s^{-1}$, respectively.

Comparison of the discharge (Figure 2(i)) and the water level (Figure 2(ii)) data demonstrate clearly that these parameters are only weakly correlated. For instance, the water level dropped drastically (over 1 m during 30 d) in March 2002 and was extremely low in April and May but the river discharge had its maximum at the end of March. The mean water level in the river mouth increased by more than 0.6 m during 15 d in June in spite of the gradually decreasing discharge. The described feature is expected, because the water level

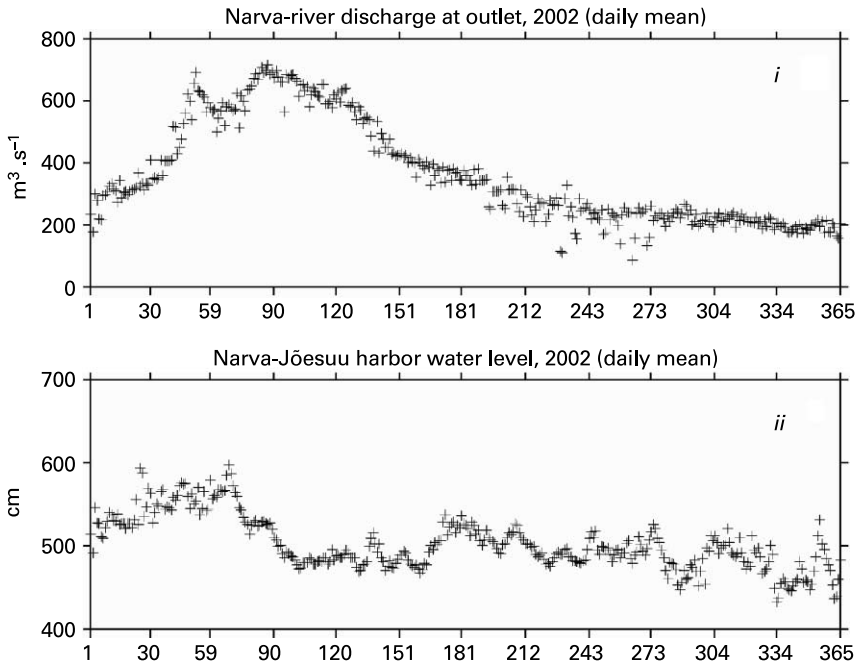

Figure 2 Hydrological parameters at the Narva River mouth: (i) river discharge and (ii) water level in the Narva-Jõesuu harbour

in the Narva-Jõesuu harbour primarily depends upon the variation of sea level in the Narva Bay (including local wind-induced sea surface variations with a typical duration of longer than a week and less than a month) but river discharge is controlled by confluence of surface water from catchment areas.

Large deposition of sand may result in considerable changes to the barrier height near the seaward end of the Narva-Jõesuu breakwater. This leads to substantial variation of the stratification and overflow conditions. The observed salinity around 2 km offshore from the river mouth (59° 28.5′N, 28° 00.5′E, water depth about 10 m, Figure 3) confirms that the river plume extends far into the bay during spring months. During autumn and winter months the sea area in close vicinity to the river mouth is stratified (Figure 4).

Within local coastal processes the surface waves dominate in the relatively shallow water near the river mouth. Since there are no long-term *in situ* wave measurements in the vicinity of the study area, the parameters of the surface waves are determined using a wave model forced by actual meteorological data. The atmospheric conditions (wind direction and speed, air temperature, etc.) are monitored at Narva-Jõesuu, at a site which is surrounded by forest and coastal cliffs (towering occasionally up over 50 m above sea level). According to the observed Narva-Jõesuu wind data in 2002, NW and SW winds dominate among moderate winds (speeds 5–9 m s^{-1}) in the river mouth area, and west and NW winds dominate among the strong winds (> 10 m s^{-1}). Moderate and strong westerly winds were frequent also during 2001 (Laanearu and Lips 2003). This is consistent with the general properties of the wind regime of the Gulf of Finland which consists of southwest and north winds dominating the whole Baltic Sea (Soomere 2003) and of local east and west winds blowing along the axis of the gulf (Soomere and Keevallik 2003) whereas southeast winds are infrequent and weak in the whole gulf. The Narva-Jõesuu coast is thus open to the dominating moderate and

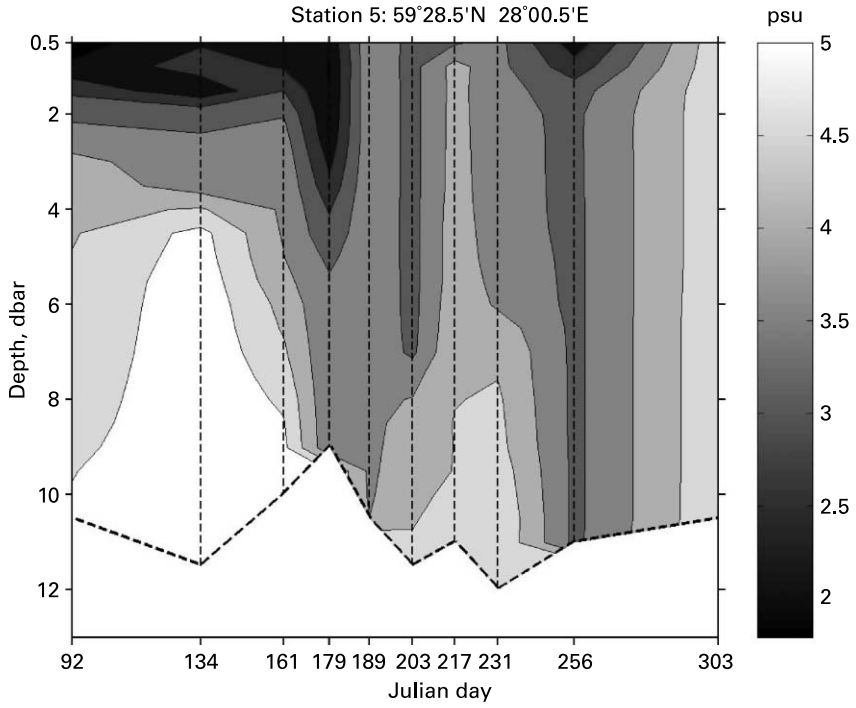

Figure 3 Salinity stratification at hydrographic station 5 (Figure 1) during the year 2002. This station is located about 2 km offshore from the river mouth where the water depth is around 10 m

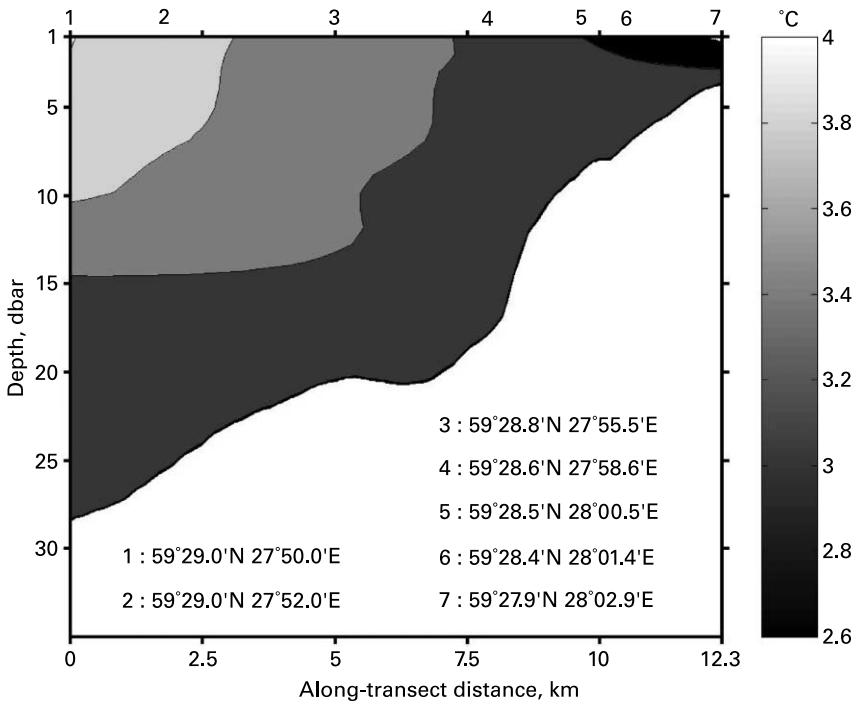

Figure 4 Transect of sea water temperature at the end of October, 2002. The locations of the hydrographic stations (1–7) are shown in Figure 1

strong westerly and north–western winds, and wind waves eventually have a strong effect on sand transport along the beach near the river outlet.

The wind wave field near the river mouth is governed by the properties of wind in the open sea. Winds that are responsible for the growth of surface waves are normally (except possibly during very strong local storms, see Launiainen and Saarinen (1982)) much stronger than those which are observed on the coast (Niros *et al.* 2002) and, therefore, should be used for wave modelling. The only observation site of the Gulf of Finland that is not affected by the presence of coasts and represents well the open sea wind properties is Kalbådagrund, a caisson lighthouse in the central part of the gulf (59°59′N, 25°36′E). The relatively high correlation between the Kalbådagrund and Narva-Jõesuu wind directions for moderate and strong winds (>5 m s^{-1}, Figure 5) and the estimated wave propagation directions suggests that the Kalbådagrund data well reflect factual properties of those open sea winds which create substantial wave loads in the Narva-Jõesuu area.

The meteorological data from Kalbådagrund are used to calculate the parameters (significant wave height, wave period and propagation direction) of wind waves in the coastal area near Narva-Jõesuu. A simplified technique of wave modelling based on cycle 4 of the WAM wave model (Komen *et al.* 1994) is employed to hindcast the wave properties near Narva-Jõesuu. The basic assumption is the fast saturation of surface waves under changing wind conditions, combined with the presumption that the wave field has a relatively short "memory" of the wind history in the area of question. This hypothesis is frequently valid for bays of the Gulf of Finland and allows reduction of long-term wave calculations to the analysis of a set of pre-computed wave patterns (Soomere 2005). Owing to relatively short fetches of the directions of dominating strong winds the typical periods of waves are relatively small (usually less than 5 s) in the whole Gulf of Finland (Soomere and

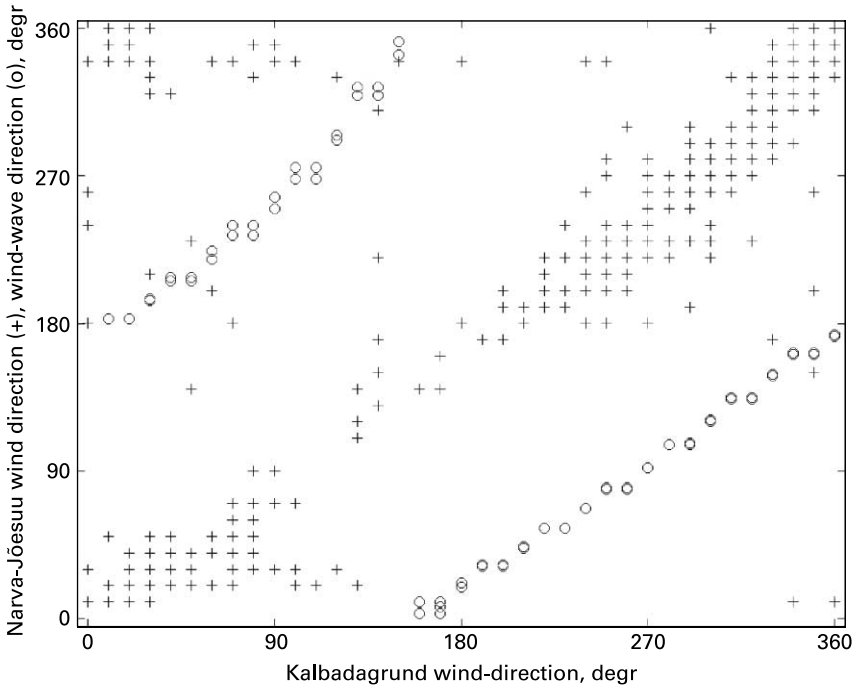

Figure 5 Scatter diagram of Kalbådagrund and Narva-Jõesuu wind directions (+), and modelled wave propagation directions (o) near the Narva-Jõesuu coast

Rannat 2003). The mismatch of the measured and hindcast wave parameters in the study area is less than 20% during a two-day measurement session at the end of October 2002. Such a good concordance suggests that the modelled wave parameters are suitable for the analysis of wind-induced processes in the Narva Bay region.

Modelling of river flow

The ratio of the sill height above riverbed (~ 4 m) to its length (~ 300 m) is sufficiently small for the flow at the Narva River mouth to be described by the shallow water equations. Upstream of the sill, the river flow can be considered as a moving layer of constant density (see Figure 6), described by open-channel flow equations:

$$u_1 \frac{\partial A}{\partial x} + A \frac{\partial u_1}{\partial x} = 0, \tag{1}$$

$$u_1 \frac{\partial u_1}{\partial x} = -g \frac{\partial \eta}{\partial x} - dF_{\text{drag}}, \tag{2}$$

where the x axis follows the river channel, $\vec{g} = (0, 0, -g)$ is the acceleration due to gravity, u_1 is the upper-layer flow velocity, η is the water level height above datum, A is the cross-sectional flow area and dF_{drag} is the boundary drag force per unit mass. The origin of the x axis is chosen at the water level measurement site at a distance L from the crest of the sill (Figure 6). For the surface elevation η at any along-stream location, we adopt the decomposition $\eta(x) = h_1(x) + h_2(x) + b(x)$, where $b(x)$ is the bottom elevation above a reference level, and $h_1(x)$ and $h_2(x)$ are the thicknesses of the out- and inflowing water layers, respectively (see Figure 6). The lower-layer velocity u_2 is assumed to be small: $u_2/u_1 \ll 1$, because of strong barotropic component in the surface layer outflowing from the river basin.

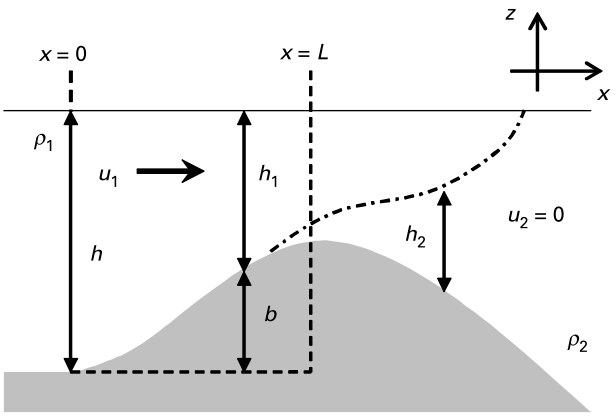

Figure 6 Schematic representation of two-layer stratification in the sill area. Notations and coordinate system of a sill flow situation. The dot-dashed curve shows the interface between the river (ρ_1) and marine (ρ_2) water

Integrating equations (1) and (2) from the upstream location $x = 0$ to any downstream location $x = \xi < L$ in the sill area (see Figure 6) yields

$$\frac{u_1(\xi)^2}{2} + gh_1(\xi) + gh_2(\xi) + gb(\xi) = \frac{u_0^2}{2} + gh_0 - \frac{1}{8}\int_0^{\xi} \frac{f_r(x)\cdot u_1(x)^2}{R_1(x)}\,\mathrm{d}x, \tag{3}$$

$$u_1(\xi)\cdot A_1(\xi) = Q_1, \quad \xi \in (0, L), \tag{4}$$

where the drag force has been expressed in the standard way in terms of a friction factor f_r, the hydraulic radius R_1 of the river channel, the flow area A_1 and the upper layer volume flux Q_1. The stream velocity and water depth at the natural river mouth (which is assumed to be located at the water level measurement site) are denoted as $u = u_1(x = 0)$ and $h = h_1(x = 0)$, respectively. Denoting the maximum height of the sill by $\Delta = b(x = L)$, dividing equation (3) by $g\Delta$ and eliminating the upper layer velocity with the use of equation (4), we reach the following integral equation for the dimensionless layer depth h_1/Δ:

$$\frac{q_L^2}{2}\left(\frac{w_L}{w(\xi)}\right)^2\left(\frac{\Delta}{h_1(\xi)}\right)^2 + \frac{h_1(\xi)}{\Delta} + \frac{b^*(\xi)}{\Delta} = B_0 - \frac{q_L^2}{8}\int_0^{\xi}\frac{f_r(x)}{R_1(x)}\left(\frac{w_L}{w(x)}\right)^2\left(\frac{\Delta}{h_1(x)}\right)^2\mathrm{d}x, \tag{5}$$

where $w(x)$ is the channel width, $w_L = w(x = L)$, $w_0 = w(x = 0)$, the height of the interface between the layers is given by $b^*(\xi) = b(\xi) + h_2(\xi)$, and q_L, B_0 are dimensionless quantities, representing volume flux and upstream-section specific energy:

$$q_L = \frac{Q_1}{g^{1/2}\Delta^{3/2}w_L}, \quad B_0 = \frac{Q_1^2}{2gw_0^2h^2\Delta} + \frac{h}{\Delta}. \tag{6}$$

Hydraulic equations (3)–(5) are similar to those developed by Pratt (1986) for the motion of a layer of fluid of uniform density over a ridge in a channel with a rectangular cross section of constant width, though, in the present case, changes of the channel width are included in the analysis. The described model accounts for the presence of a dense intrusion layer in the sill area, the occurrence of which depends both on the water level and river discharge rate.

The water depth at a particular section of the river depends, in addition to the volume flux and bottom height, also on the channel geometry and frictional boundaries. Solutions of equation (5) can be presented locally at any section $x = (0, L)$ provided the quantities q_L, B_0 are known. In the simplest case the dimensionless volume flux can be set to a constant

$q_L = 0.08$ (this corresponds to typical values of $Q_1 = 400\,\mathrm{m^3\,s^{-1}}$, $w_L = 200\,\mathrm{m}$ and $\Delta = 4\,\mathrm{m}$) and the dimensionless energy parameter

$$B_{0L} = B_0(x = L) = B_0 - \frac{q_L^2}{8}\int_0^L \frac{f_r(x)}{R_1(x)}\left(\frac{w_L}{w(x)}\right)^2\left(\frac{\Delta}{h_1(x)}\right)^2 \mathrm{d}x$$

is given for the sill section. Thus solutions for h_{1L}/Δ and h_{2L}/Δ can be calculated by equation (5).

Figure 7 presents the solution branches corresponding to the sub-critical (upper branch) and super-critical (lower branch) flow states of the upper layer, respectively, occurring on top of the quiescent lower layer ($u_2 = 0$). The hydraulically controlled solutions corresponding to $Fr^2 = q_L^2(\Delta/h_{1L})^3 = 1$ represent smooth transitions from the sub-critical to super-critical flow state. The sub-critical solutions are only relevant, because flow in the Narva River mouth area is characterized by small open-channel Froude numbers ($Fr < 1$) even during strong outflows of the river water in spring months.

An important parameter in the analysis of stratified flow at the sill section is the internal Froude number $F_1^2 = (q_L^2/(1-r)) \cdot (\Delta/h_{1L})^3$ of the upper layer flow for the arrested lower layer case (called reduced-gravity flow). The (internally) critical condition for such a flow is $F_1 = 1$. The relevant solutions for observed density ratio r, limits of which in the Narva River mouth are indicated by dashed lines in Figure 7. Internally controlled flow situations are discussed in the fifth section. Unlike one-layer flow, the sub- and super-critical solutions of the two-layer problem can change branch not only due to variations in channel geometry. The internal hydraulic transition cannot occur at the branch-point of the upper layer but must be sub-critical in the sense of single-layer flow (Laanearu and Davies 2007).

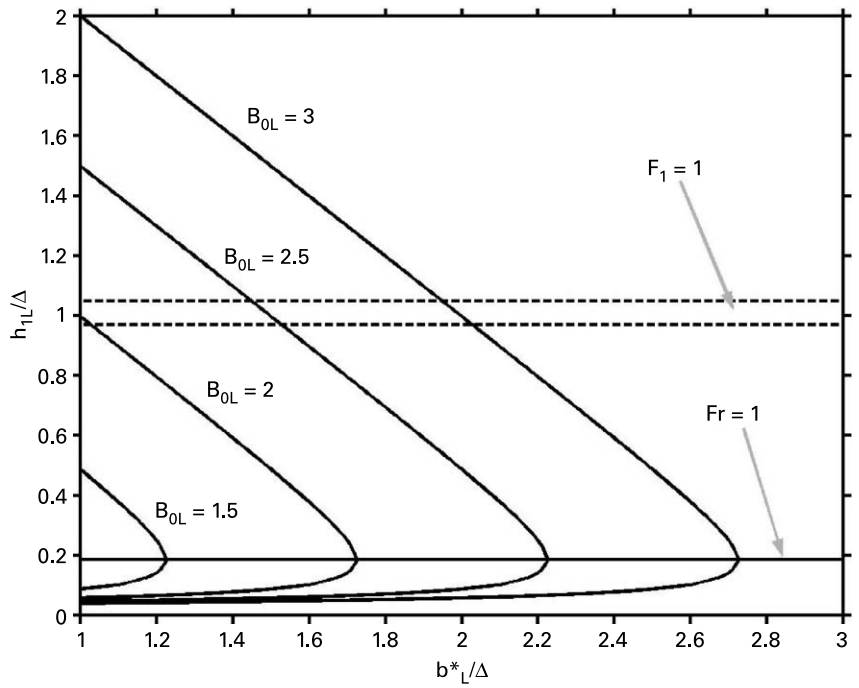

Figure 7 Solution branches for the dimensionless height h_{1L}/Δ of the river flow with respect to the dimensionless interface height b_L^*/Δ (solid curves), branch-point solutions of the open channel flow corresponding to $Fr = 1$ (solid straight line) and critical condition of two-layer flow with arrested lower layer (dashed lines, $F_1 = 1$)

Morphodynamic relationships

The bathymetry of the sandy coast near the Narva River mouth changes continuously. An integrated treatment of sand movements caused by both waves and currents is required in order to predict such changes. A distinction is often made between cross- and long-shore sediment transports (Van Rijn 1993). On the one hand, the comparatively large discharge from the Narva River eventually constitutes the primary agent for the reduction in height of any sand bar feature at the river mouth and the accompanied offshore sediment transport. On the other hand, the long-shore transport processes that are responsible for gradual refilling of the sand bar area with coastal sediments are controlled primarily by the wave-induced velocity field in the near-shore zone.

The bed-load transport of sediments in a so-called "energetic" environment can be estimated on the basis of the "stream power" required to move the sediment volume (cf. Bagnold 1966). The transport, induced by the river flow, can be characterized by a current friction factor f_r (introduced in equation (3)). According to Jonsson (1966) the bottom shear stress due to the river current is $\tau_r = (1/8) f_r \rho u^2$, where $f_r = f_r(\mathrm{Re}_c)$ is a function of the channel Reynolds number $\mathrm{Re}_c = uR/\nu$ and ν is the coefficient of kinematic viscosity. In the Narva River mouth the flow reveals turbulent character, viz. $\mathrm{Re}_c \sim 10^6$.

The cross-shore sand-volume flux per unit width $q_{cs} (= \delta u_s)$ (where u_s is the cross-shore velocity scale of the bulk sediment volume and δ is the thickness of sediment volume in Figure 8 for the case with $\alpha = 0$), can be expressed in terms of the river flow stream power $\tau_r u$ and the proportion e_f (the efficiency factor) of this power available to move the sediment as follows:

$$q_{cs} = \frac{\tau_r u_{1L} \cdot e_f}{(\rho_s - \rho) \varepsilon g \ \tan \ \Phi}, \tag{7}$$

where ρ_s is sediment grain density, ρ is the water density, ε is the coefficient of sediment volumetric concentration and Φ is the angle of repose of the sediment representing the coefficient of internal friction ($\tan \ \Phi$). The bed load transport equation (7) relates the along-channel sediment flux to the mechanical work needed to move an entire horizontal "layer" of sediment at the sill summit.

According to Jonsson (1966) the bottom shear stress τ_w due to the unsteady, wave-induced velocity field can be defined in terms of a wave friction factor f_w in the conventional manner as $\tau_w = (1/2) f_w \rho v^2$. If the wave Reynolds number $\mathrm{Re}_w = \mathrm{v} A_w / \nu \geq 3.3 \times 10^4$, the wave-induced flow may be regarded as fully turbulent. The wave friction factor for hydraulically smooth flow can then be predicted, using the physical roughness relationship $k_n = 30\nu/(9u_*)$, where u_* is the frictional velocity (Grant and Madsen 1986). The maximum wave-induced near-bed orbital velocity v can be calculated from linear gravity-wave theory as $\mathrm{v} = a\omega \ \sinh^{-1}(kD)$, where ω is the angular frequency, k is the wavenumber, a is the

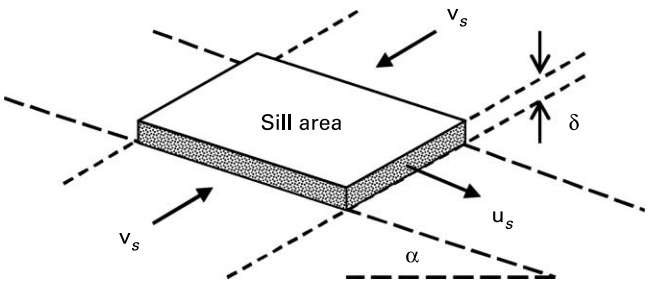

Figure 8 Schematic representation of a sloping coastal slab of sediments. Directions of sediment motion are indicated by cross-shore (u_s) and long-shore (v_s) velocity

significant wave amplitude (half of the significant wave height) and D is the undisturbed water depth. The bottom excursion amplitude is $A_w \equiv \mathrm{v}/\omega$.

The effect of the waves on sediment motion in shallow water before the surf zone depends on the angle between the wave crests and the bottom isobaths and is greatest if this angle is $\pi/4$ (Millard 1997). Waves approaching the Narva-Jõesuu beach from the open sea (see Figure 1) are characterized by the angle φ measured clockwise between the direction to the North and the wave vector (i.e. $\varphi \leq \pi/4$ and $\varphi \geq 5\pi/4$). The sediment-volume flux $q_{vs}(= \delta \mathrm{v}_s)$ (where v_s is the long-shore velocity scale of the sediment volume) per unit width on a sloping coast (given by an angle α in Figure 8) can be estimated as

$$q_{vs} = \frac{\tau_w v \cdot e_f}{(\rho_s - \rho)\varepsilon g \ \cos \ \alpha \ \tan \ \Phi} |\cos(\pi - 2\varphi)|. \tag{8}$$

Using the mass conservation principle for a control volume of sill area the changes in the height of the sand bar can be calculated iteratively resulting from both the erosion and deposition as

$$\Delta^{i+1} = \Delta^i + \varsigma_1 \frac{K_1 \tau_w^i}{Y_s \varepsilon \ \cos \ \alpha} |\cos(\pi - 2\varphi^i)| - \varsigma_2 \frac{K_2 \tau_r^i}{Y_s \varepsilon}, \tag{9}$$

where (K_1, K_2) are morphodynamic coefficients and $Y_s = (\rho_s - \rho)g$ is the submerged weight per unit volume of bottom sediments. The operators $(\varsigma_1, \varsigma_2)$ specify whether the sand bar is being eroded by the river flow $(\varsigma_1 = 1, \varsigma_2 = 0)$ or being filled by sediment due to the wave-induced motions $(\varsigma_1 = 0, \varsigma_2 = 1)$. Such a switching between regimes of erosion and replenishment of the river mouth sill represents the above-discussed separation in time for two dominating coastal processes in the area of question.

The sediments at the Narva River mouth consist mostly of sand but also include some small amount inorganic (e.g. clay, gravel) and organic substances. The experimentally estimated submerged weight is $Y_s = 15\,631\,\mathrm{kg/(m^2\ s^2)}$ and the coefficient of sediment volumetric concentration is $\varepsilon = 0.63$. The region-specific coefficients (K_1, K_2) depend on the coefficients of internal friction, the efficiency factors and the ratios $(\mathrm{v}/\mathrm{v}_s)$,$(u/u_s)$, respectively. The efficiency factor e_f ranges between 0.1 and 0.2 in water. The coefficient of internal friction tan $\Phi \sim 0.6$ for sand (Bagnold 1966). In order to close the bed-load transport problem one has to specify the values of (K_1, K_2). Their choice (in first approximation treated as constants) should be consistent with the temporal and spatial scales of the observed bottom height variation at the sand bar area.

Analysis and results

The developed morphodynamical model contains two region-specific coefficients in equation (9) which can be determined empirically from the bed-load measurements. However, due to a lack of information about sand recycling at the Narva River mouth, in this study these coefficients are estimated on a best-fit basis according to the observed bathymetrical and hydrological parameters and the modelled surface wave time series.

A particularly important step in solving equation (9) consists in determination of whether the cross- or long-shore sand motion dominates in the sand-bar area at a certain time instant. This is a nontrivial problem, because the separation of the river flow from the bottom boundary (see Figure 6) and the occurrence of an intruding saline layer (usually accompanied by low flow velocities and domination of wave-induced hydrodynamic loads) are related to joint variations in the sea level and the river discharge. Observations at the mouth of the Narva River indicate the presence of a highly stratified front, the occurrence of which depends upon the strength of the river discharge and hydrodynamic processes in the bay (Laanearu and Lips 2003). Such fronts can be parametrized within a two-layer

framework (Laanearu and Davies 2007). The properties of exchange flows are described in terms of the composite Froude number $G = \sqrt{F_1^2 + F_2^2}$, where $F_i^2 = u_i^2/(g'h_i)$ are the densimetric Froude numbers of the layers, where $i = 1$ corresponds to the upper and $i = 2$ to the lower layer, $g' = g(1 - r)$ is the reduced gravity acceleration and $r = \rho_1/\rho_2$ represents the density ratio of the river (ρ_1) and sea (ρ_2) water.

For an idealized case of a typical river front, the lower layer is arrested ($u_2 = 0$) and the composite Froude number $G = F_1$. Since the value of the internal Froude number is exactly one at the front, supercritical values $G > 1$ occur seaward of the front, where stratification is present (see Figure 6). Therefore, the value of G indicates whether the flow at the Narva River mouth is stratified or not, and allows us to determine the instantaneous values of the flow-regime operators $(\varsigma_1, \varsigma_2)$ in equation (9). The separation can therefore be done by tracking whether the value of the internal Froude number F_1 of the upper layer satisfies either $F_1^2 > 1$ or $F_1^2 \leq 1$.

A series of trial runs shows that a solution to the morphodynamic problem can be obtained for reasonable variations of the water depth at the barrier and at the natural river mouth using values $K_1 = 60$ and $K_2 = 40$ in equation (9). The distance between the natural river mouth and the sill, the flow width at the river mouth ($x = 0$) and at the barrier ($x = L$) are taken as $L = 400\,\text{m}$, $w_0 = 100\,\text{m}$ and $w_L = 200\,\text{m}$, respectively. The time series of the estimated bottom stresses caused by wind waves and river flow for the period in question, obtained using the observed hydrological and meteorological data presented in Figures 2 and 5, together with approximations developed in previous sections, are shown in Figure 9. As expected, the wave-induced stress has strong temporal variations, though its magnitude generally is of the same order as that of the more slowly varying river-flow-induced stress. The bottom stress induced by the waves is comparatively large during winter, early spring and late autumn months. In contrast, the specific-energy loss (proportional to the river

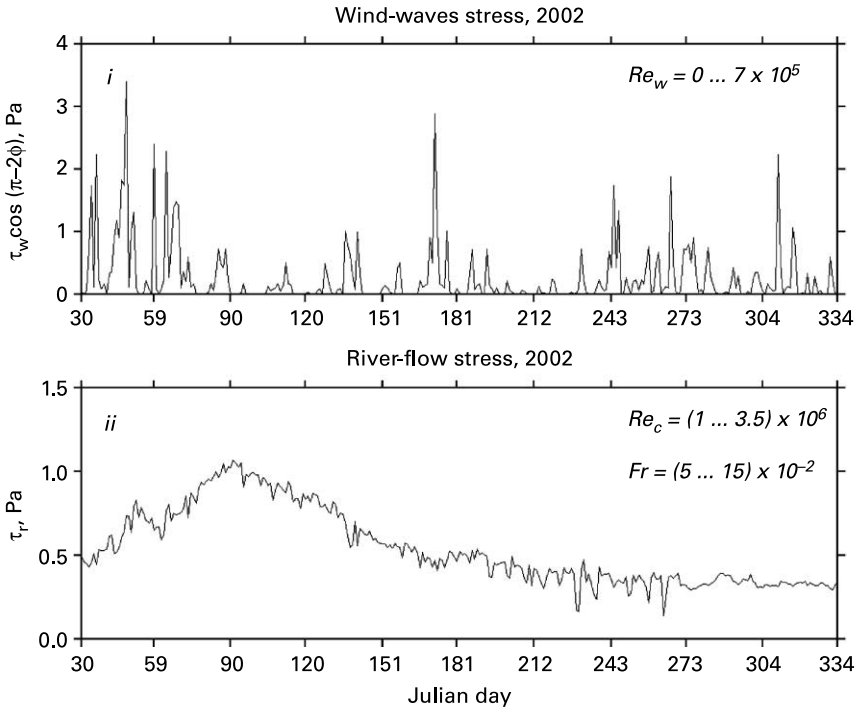

Figure 9 Modelled wave-induced bottom stress at the Narva-Jõesuu coast (i) and river-flow-induced bottom stress at the sill area (ii)

bottom stress) of the cross-shore current is comparatively large during spring and early summer months. Figure 9 demonstrates clearly that the correlation between the river- and wave-induced stresses driving the cross- and along-shore sediment transport, respectively, is really weak.

Figure 10 shows the barrier height calculated using equation (9). For each point on the plot, the internal Froude number F_1 values are also indicated, in order to classify the variation with time in the hydraulic regime. (Note that Figure 10 shows only the portion of the annual record during the ice-free period.) The calculated total variation of the barrier height ($\Delta_{37} - \Delta_{168}$) is around 0.4 m and the difference in height during the early spring and late fall ($\Delta_{37} - \Delta_{334}$) is less than 0.2 m. The subscript indicates the particular Julian day.

The range of values of (K_1, K_2) is obviously restricted if realistic water depths are to be obtained in the river-mouth area. The above values of (K_1, K_2) and a constant ratio $K_1 : K_2 = 3 : 2$ thus provide a reasonable choice for the model calculation for the Narva River mouth case. With this choice, the model represents well the balanced situation between the river-flow-induced erosion and wave-induced deposition of sediments in the area of question. The modelled sill-height variation depends on the choice of the region-specific coefficients, though even quite a large variation of these coefficients still yields reasonable results. The variation of $\pm 50\%$ of the coefficient K_1 yields the absolute change of the barrier height $\Delta_{334} = 4.18$ m by ± 0.14 m. The analogous variation of K_2 gives the change of Δ_{334} by ± 0.18 m. The above variation of K_1 has no significant effect on the total variation of the barrier height $\Delta_{37} - \Delta_{168}$, but the analogous variation of K_2 yields the total variation of the barrier height in the range $(0.2, 0.6)$ m.

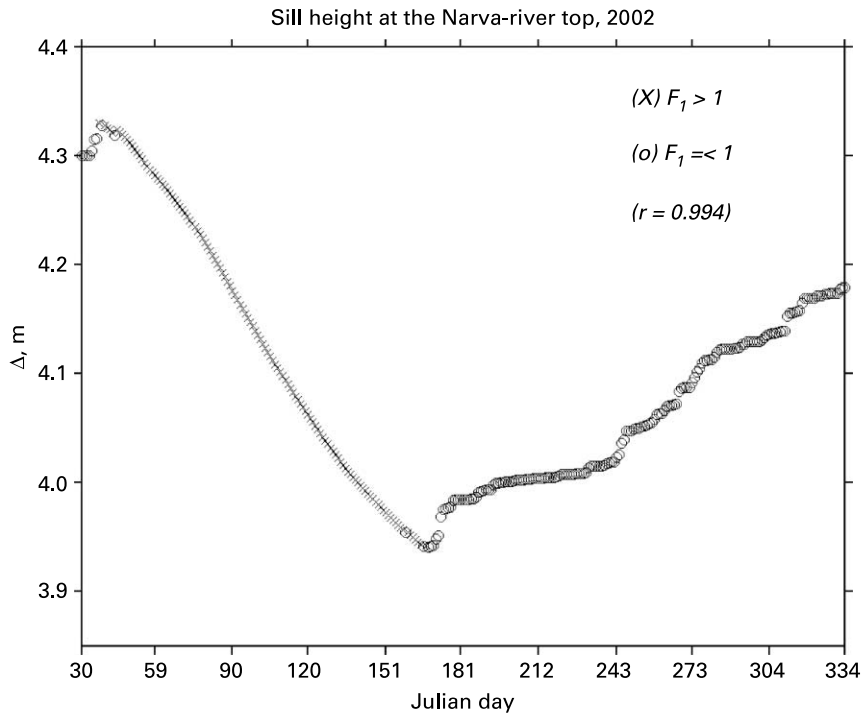

Figure 10 Modelled variation of the sill height at the seaward end of the Narva-Jõesuu breakwater. The values of internal Froude number are indicated for uniform (x) and stratified (o) flow situations

An expected feature of the results presented in Figure 10 is that the modelled flow reveals a unidirectional structure predominantly during the spring and early summer months, when the cross-shore bottom stress is large due to a comparatively low sea level and large runoff from the river. The water level rise occurring in June (see Figure 2) yields considerable changes in the modelled flow structure and results in the change of a one-layer ($F_1 > 1$) to a two-layer flow situation ($F_1 \leq 1$) for the second half of the summer. The latter structure persists during the autumn and winter months when windstorms were frequent and the surface waves had a considerable impact on the long-shore sediment motion.

It is also interesting to notice that a ratio $K_1/K_2 = 1.5$ coincides with the ratio of the distance of the barrier from the coastline and the width of the river mouth. Using approximate values $e_f = 0.12$, $\tan \Phi = 0.6$, the bulk annual cross-shore transport is around 50.8×10^6 kg, whereas its daily values vary between 0 and 0.67×10^6 kg. The bulk long-shore transport of sediments replenishing the sill region was around 53% of the annual cross-shore transport. The reduction of the barrier height is naturally limited by the occurrence of stratification; though during winter months the river stream is separated from the barrier summit because of the intruded saline layer that cancels the erosion of the sand bar by the river flow.

Conclusions and discussion

The modelling study demonstrated that the changes of underwater sand bar in the Narva River mouth had a clear annual cycle for 2002, resulting from the sand motion due to river flow and surface waves. The maximum variation of the barrier height was around 0.4 m and the difference in height during the year was less than 0.2 m. A regionally important aspect of the morphodynamical problem is that the water depth in the vicinity of the seaward end of the breakwater is considerably smaller than that in the natural river mouth. This is the effect of long-term coastal processes caused by the breakwater and indicates that sediment deposition inside the river basin is less important for sediments processes at the coast. The river flow induces the erosion that dominates only in the area of the sand bar. The modelled flow at the Narva River mouth (with the external Froude number Fr ranging between 0.05 and 0.15) showed that internal dynamics is important to understand the controlling mechanism for stratification in a mouth of a river. According to the present modelling study, the height of the sand bar is the lowest in mid-summer when also relatively low water level occurs. An occurrence of a high sea-level event in this situation may cause the river flow velocity over the bar to reduce considerably. This may result in an intrusion of sea water over the bar and in the generation of associated flow stratification. The modelled flow conditions reveal that the stratified flow structure exists primarily during the period of frequent occurrence of storms that can change conditions of the relatively high water level in the area in question. The estimated internal Froude number for 2002 corresponded to the internal hydraulic conditions that can be related to the net exchange flow (see Laanearu and Davies 2006).

In the Narva River mouth, the channel Reynolds number Re_c ranged between 1×10^6 and 3.5×10^6 near the seaward end of the breakwater; constituting that the river flow is turbulent. An accurate representation of the physics of both the flow and sediment transport processes in the portion of the river upstream of the sand bar requires an ability to predict the geometrical characteristics of the bed forms. The effects of wind waves on morphodynamic changes are treated in this study independently. The wave's Reynolds number Re_w in the coastal zone ranged between 0 and 7×10^5, and the frictional factor has been calculated for a hydraulically smooth, turbulent wave boundary layer case (cf. Madsen and Grant 1976). In the river-mouth area, where the river outflow is characterized by a very high Reynolds number, it is likely that the surface waves, through their interaction with the river outflow,

can have a different effect on the sediment transport than for a coastal area remote from the river outflow.

The quasi-stationary approximation for hydraulic modelling employed in this study is justified if flow adjustment processes are rapid compared with the timescale of changes in the forcing conditions. It has been shown that the overall changes of the environmental parameters were comparatively slow for this case and the requirements for quasi-stationary flow in the river mouth are well satisfied. Laboratory experiments (cf. Cuthbertson *et al.* 2006) on unsteady, two-layer and exchange flow over a slowly descending barrier support this approach. "High-frequency" components of forcing functions such as instantaneous water level (due to sudden windstorms) or discharge fluctuations (for example, those associated with the break of a river dam), can have irreversible effects on coastal changes and are not in the scope of the present study.

A key issue for future study is the adjustment of bi-directional flow to realistic bathymetric conditions and inclusion of roughness elements in the hydraulic model. A feasible way toward progress in this area may consist in making a wider use of the concept of stratified flow hydraulics in non-rectangular channels (Laanearu and Davies 2007). The success of this approach depends on parametrization of the two-layer flow in terms of non-standard internal Froude numbers, which can be related to internally critical conditions of natural inlets.

Acknowledgements

This study has been supported by several grants from: (i) Tallinn University of Technology (Targeted Financing 0142514s03), (ii) Estonian Science Foundation (Grant 5762), (iii) Institute of Marine Systems and (iv) UK Engineering and Physical Sciences Research Council. The author is grateful for the technical assistance provided by crews of the vessels SAKA (Toila) and RVK001 (Narva-Jõesuu).

References

Alenius, P., Myrberg, K. and Nekrasov, A. (1998). The physical oceanography of the Gulf of Finland. *A. Review. Boreal. Env. Res.*, **3**, 97–125.

Bagnold, R. (1966). *An Approach to the Sediment Transport Problem from General Physics*. Technical report. Geophysical Survey Professional Paper 422-I, Washington, DC.

Baines, P.G. (1998). *Topographic Effects in Stratified Flows. Cambridge Monographs in Mechanics*, Cambridge University Press, Cambridge.

Coates, M.J., Guo, Y. and Davies, P.A. (2001). Laboratory model studies of flushing of trapped salt water from a blocked tidal estuary. *J. Hydraul. Res.*, **39**(6), 601–609.

Cuthbertson, A.J.S., Davies, P.A., Coates, M.J. and Guo, Y. (2004). A modelling study of transient, buoyancy-driven exchange flow over a descending barrier. *Environ. Fluid Mech.*, **4**, 127–155.

Cuthbertson, A.J., Laanearu, J. and Davies, P.A. (2006). Buoyancy-driven two-layer exchange flows across a slowly submerging barrier. *Environ. Fluid Mech.*, **6**, 133–151.

Grant, W.D. and Madsen, O.S. (1986). The continental shelf bottom boundary layer. *A. Rev. Fluid Mech.*, **18**, 265–305.

Jonsson, I.G. (1966). Wave boundary layers and friction factor. *Proc. 10th Int. Conf. on Coastal Engineering, Tokyo, Japan*, ACSE, New York. pp. 127–148.

Kalkwijk, J.P.Th. and Koppel, T.A. (1985). Experiments on unsteady separating flow in an open channel. In: *Proc. 21st IAHR Congress, Melbourne, Australia*. pp. 102–108.

Komen, G.J., Cavaleri, L., Donelan, M., Hasselmann, K., Hasselmann, S. and Janssen, P.A.E.M. (1994). *Dynamics and Modelling of Ocean Waves*, Cambridge University Press, Cambridge.

Laanearu, J. and Davies, P.A. (2006). Barotropic effects of surface layer on water exchange through horizontal channels with quadratic-shape cross-sections. In G.N. Ivey (Ed.), *Proc. 6th International Symposium on Stratified Flows*, School of Environmental Systems Engineering, The University of Western Australia, Perth. pp. 336–341.

Laanearu, J. and Davies, P. (2007). Hydraulic control of two-layer flow in "quadratic"-type channels. *J. Hydraul. Res.*, **45**(1), 3–12.

Laanearu, J. and Lips, U. (2003). Observed thermohaline fields and low-frequency currents in Narva Bay. *Proc. Estonian Acad. Sci. Engng.*, **9**(2), 99–106.

Largier, J.L., Slinger, J.H. and Taljaard, S. (1992). The stratified hydrodynamics of the Palmiet – a prototype bar built estuary. In D. Prandle (Ed.), *Dynamics and Exchanges in Estuaries and the Coastal Zone*, American Geophysical Union, Washington, DC. pp. 135–153.

Launiainen, J. and Saarinen, J. (1982). Examples of comparison of wind and air-sea interaction characteristics on the open sea and in the coastal areas of the Gulf of Finland. *Geophysica*, **19**, 33–46.

Madsen, O.S. and Grant, W.D. (1976). Quantitative description of sediment transport by waves. *Proc. 15th International Coastal Engineering Conference*, American Society of Civil Engineers, Reston, VA. pp. 1093–1112.

Millard, K. (1997). Computer modelling and Earth observation: providing data for coastal engineering. In A.P. Cracknell and E.S. Rowan (Eds.), *Physical Processes in the Coastal Zone, Computer Modelling and Remote Sensing*, SUSSP Publications, Dundee. pp. 295–314.

Niros, A., Vihma, T. and Launiainen, J. (2002). Marine meteorological conditions and air-sea exchange processes over the northern Baltic Sea in 1990s. *Geophysica*, **38**, 59–87.

Pratt, L. (1986). Hydraulic control of sill flow with bottom friction. *J. Phys. Oceanogr.*, **16**, 1970–1980.

Protasjeva, M. and Eipre T. (Eds.) (1972). *Resources of the Surface Water of the USSR. Baltic Region. Estonia*. Gidrometeoizdat, Leningrad (in Russian).

Soomere, T. (2003). Anisotropy of wind and wave regimes in the Baltic Proper. *J. Sea Res.*, **49**, 305–316.

Soomere, T. (2005). Wind wave statistics in Tallinn Bay. *Boreal Environ. Res.*, **10**, 103–118.

Soomere, T. and Keevallik, S. (2003). Directional and extreme wind properties in the Gulf of Riga. *Proc. Estonian Acad. Sci. Engng.*, **9**(2), 73–90.

Soomere, T. and Rannat, K. (2003). An experimental study of wind waves and ship wakes in Tallinn Bay. *Proc. Estonian Acad. Sci. Engng.*, **9**(3), 157–184.

Van Rijn, L.C. (1993). *Principles of Sediment Transport in Rivers, Estuaries and Coastal Sea*, Aqua Publications, Amsterdam.

Wübber, C. and Krauss, W. (1979). The two-dimensional seiches of the Baltic Sea. *Oceanol. Acta*, **2**, 435–447.